W. Kreil; W. Schnitzler; Gerhard Schweizer

Transfer function measurements with statistical methods by means of digital computation

Kybernetika, Vol. 4 (1968), No. 3, (226)--245

Persistent URL: http://dml.cz/dmlcz/124630

KYBERNETIKA ČÍSLO 3, ROČNÍK 4/1968

Transfer Function Measurements with Statistical Methods by means of Digital Computation

W. KREIL, W. SCHNITZLER, G. SCHWEIZER

The article describes methods of processing data which represent measurements taken from a physical system where stochastic components are involved. Digital computer application is discussed in some detail, with special emphasis on programming for maximum processing speed.

I. INTRODUCTION

The dynamic characteristics of linear systems, especially linear constant parameter systems, can be described by frequency response functions. For physically realizable and stable systems, the frequency response function of a system may replace the transfer function with no loss of information.

Extended developments of aerospace systems require the determination of the frequency response functions of many subsystems for the judgement of the overall performance. In some cases, appropriate transfer functions can be obtained by analytical procedures. However, there are many examples where the determination of the transfer function or frequency response by analytical methods is presently beyond the state of the art. This is particularly true for physiological systems.

Because of these difficulties it is common to determine the frequency response of linear systems by empirical methods. The most straightforward approach is to subject the system to a sinusoidal input and to measure the output-magnitude and -phase as the stimulus frequency is varied.

There are many situations during the development of aerospace systems where it is not possible to apply sinusoidal stimuli. This applies to the majority of measurements during normal operation (that means in-flight measurements). In this case, it is possible to establish frequency response functions by means of inherent or artificial random input. Quite often the problems are further complicated because open-loop measurements are not feasible. The determination of open-loop transfer functions by means of closed-loop measurements requires usually high accuracy.

The development of a variety of aerospace vehicles and the necessity of processing enormous quantities of test data especially from flight tests have initiated the use of digital computer programs to determine transfer functions with statistical methods at the Dornier GmbH, Friedrichshafen. Hence the necessary equipment and the computer programs have been carefully planned, great amount of data can be processed conveniently in very short time. System performance, malfunctions of subsystems and parameter identification are investigated by means of transfer function and power density spectra measurements.

II.1 Data Acquisition

The first step of the data processing procedure is obviously the data acquisition. The Dornier Installations can be used to convert the physical parameters into voltages and store them on magnetic tapes either in analog or digital format. The tape-recorders can be installed on board of any vehicle or at ground stations. Signals to remote stations are transmitted via telemetry (Fig. 1).

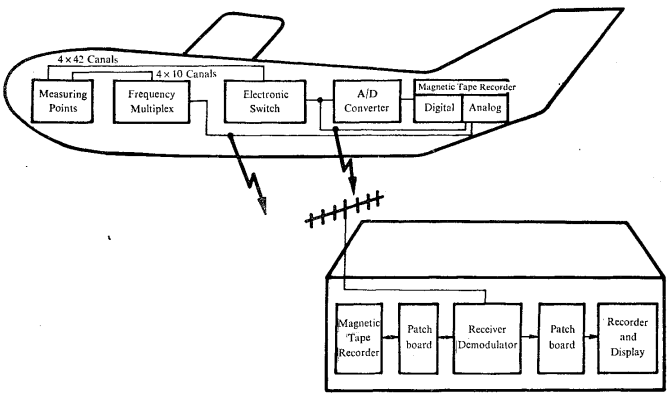

Fig. 1. Data acquisition equipment of the Dornier GmbH.

Computer programs and the necessary equipment are available to feed the data in any analog or digital format from tapes into the digital computer.

On line data acquisition of analog electrical signals from simulator or rig tests is feasible. For this purpose a program can be used to sample 20 different signals in a specified way in time intervals less than 1 millisecond under computer control. Fig. 2 shows the Dornier Hybrid Computer which is used for data acquisition and processing.

II.2 Data Processing of Weakly Stationary Processes

Fig. 3 shows a block diagram for processing weakly stationary data with the Dornier Installation. If there is some indication that the data could be random, the process is plotted for a first short inspection. Then the data are tested for station-

Fig. 2. Dornier GmbH hybrid computer installation.

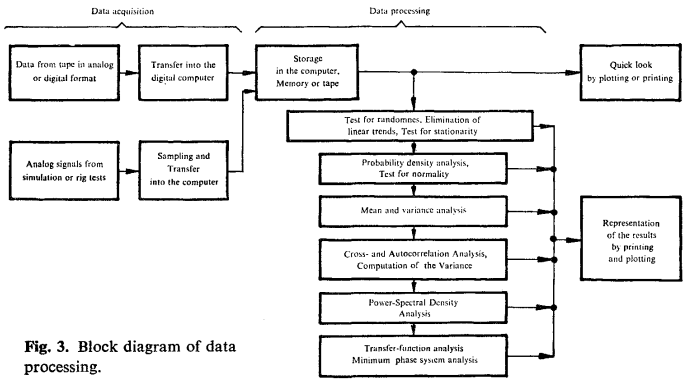

Fig. 3. Block diagram of data processing.

arity, for randomness and possible linear trends. The techniques for determining whether the data are stationary and random are straightforward and rather simple.

The sampled data are divided into several sequences. Then the statistical properties for these sequences are computed by time averaging. If these statistical properties

do not vary significantly, the process is considered as stationary. Under two assumptions a sufficient stationarity test for a sequence is available by computation of the mean- and the mean-squarevalue (or the variance):

a) The process has a Gaussian probability density function;

b) The correlation function is stationary if the variance is stationary.

These assumptions are usually valid. Furthermore the experience shows that power density spectra and autocorrelation analysis yield good results, even if the processes are weakly stationary. In the case where any trend of the mean values can be assumed, linear correction for this slight nonstationary and nonrandom effects is provided in the following way.

Ususally the data are divided into three sequences. If the three means indicate a nonstationary trend as shown in Fig. 4, where the individual means have increasing values, correction is provided. For this purpose only the stochastically changing part of the data about the straight line

$$X_G(i) = i \,.\, \alpha + \beta \quad (i = 1, 2, 3, \ldots, N) \tag{1}$$

is considered within the analysis (Fig. 4).

$$\alpha = \frac{3}{2N}(\bar{x}_0 - \bar{x}_u)\,, \tag{2}$$

$$\beta = \tfrac{1}{4} \,.\, (5\bar{x}_u - \bar{x}_0)\,, \tag{3}$$

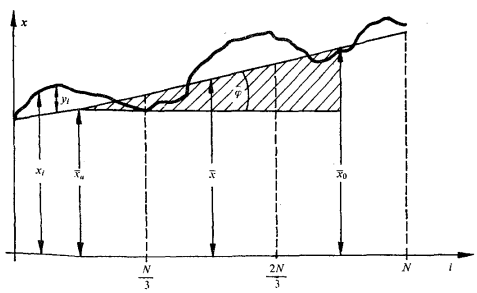

Fig. 4. Elimination of mean and linear trend.

$\bar{x}_u$ is the mean of the first third of the data, $\bar{x}_0$ the mean of the last third,

$$\bar{x}_u = \frac{3}{N} \sum_{i=1}^{N/3} x_i\,, \tag{4}$$

$$\bar{x}_0 = \frac{3}{N} \sum_{i=1+2N/3}^{N} x_i \,. \tag{5}$$

The random ordinates about the straight line are to be

$$y_i = x_i - \bar{x} + \frac{3}{2N}\left(\frac{N}{2} - i\right)(\bar{x}_0 - \bar{x}_u) \,. \tag{6}$$

If random processes with trends are corrected in this way, large distortions at low frequencies and particularly at zero frequency are avoided. The correction for linear trends makes only sense in the presence of such a trend.

Before analyzing these data, only the overall mean value will be subtracted.

$$y_i = x_i - \bar{x} \quad \text{with} \quad \bar{x} = \frac{1}{N} \sum_{i=1}^{N} x_i \,. \tag{7}$$

In the data contain sinusoidal components, they can be easily detected by the auto-correlation function.

Experience has shown that in almost any practical test the probability distribution can be approximated by the normal (Gaussian) distribution. The validity of this assumption is usually proved by a chi-square goodness-of-fit test [1].

II.3 Details of Digital Computer Techniques for the Determination of Correlation Functions and Power Density Spectra

The auto- and crosscorrelation function is obtained by means of Eqs. (8) and (9)

$$\Phi_{xx}(\tau) = \lim_{T \to \infty} \frac{1}{2T} \int_{-T}^{+T} x(t) \,.\, x(t + \tau)\, \mathrm{d}t \,, \tag{8}$$

$$\Phi_{xz}(\tau) = \lim_{T \to \infty} \frac{1}{2T} \int_{-T}^{+T} x(t) \,.\, z(t + \tau)\, \mathrm{d}t \,. \tag{9}$$

The auto correlation function is even:

$$\Phi_{xx}(\tau) = \Phi_{xx}(-\tau) \,. \tag{10}$$

By substitution $t + \tau = t'$ in Eq. (9) one obtains for the crosscorrelation function the relation

$$\Phi_{xz}(-\tau) = \Phi_{zx}(\tau) \,. \tag{11}$$

For digital calculations the data have to be sampled. Therefore only discrete values for the correlation functions can be computed. The data $\{x\}$ and $\{z\}$ are only available for positive times. If one has the data available for a length of $N \,.\, \Delta t$, good accuracy can be expected for correlation times $M \,.\, \Delta t$ where $M \leqq 0{,}1N$.

For numerical computations, Eqs. (8) and (9) become

$$\Phi_{yy}(m) = \frac{1}{N-m} \sum_{i=1}^{N-m} y_i \cdot y_{i+m}, \quad 0 \leqq m \leqq M, \tag{12}$$

$$\Phi_{yv}(m) = \frac{1}{N-m} \sum_{i=1}^{N-m} y_i v_{i+m}, \quad 0 \leqq m \leqq M, \tag{13a}$$

$$\Phi_{yv}(m) = \frac{1}{N-|m|} \sum_{i=1}^{N-|m|} v_i \cdot y_{i+|m|}, \quad -M \leqq m < 0. \tag{13b}$$

Hereby the data $\{x\}$ and $\{z\}$ have been converted to the normalized data $\{y\}$ and $\{v\}$ by Eq. (6) or (7).

The correlation functions computed by means of Eqs. (12) and (13) can be used as an unbiased estimate of the true value. For the error analysis the variance of the correlation function will be computed

$$\sigma^2_{xx}(m) = E\{(\Phi_{xx}(m) - \bar{\Phi}_{xx}(m))^2\}, \tag{14}$$

$$\sigma^2_{xz}(m) = E\{(\Phi_{xz}(m) - \bar{\Phi}_{xx}(m))^2\}. \tag{15}$$

If one determines the relations (14) and (15) explicitly and assumes normal probability density functions of the data $\{x\}$ and $\{z\}$, the following relations will be obtained:

$$\sigma^2_{xx}(m) = \frac{2}{(N-m)^2} \sum_{k=0}^{N-m-1} (N-m-k-1 \cdot \left[\Phi_{xx}(k) + \Phi_{xx}(k+m)\,\Phi_{xx}(k-m)\right], \tag{16}$$

$$\sigma^2_{xz}(m) = \frac{2}{(N-m)^2} \sum_{k=0}^{N-m-1} (N-m-k-1) \cdot \left[\Phi_{xx}(k)\,\Phi_{zz}(k) + \Phi_{xz}(k+m)\,\Phi_{xz}(-k+m)\right]. \tag{17}$$

Eqs. (16) and (17) cannot be evaluated in their present form since the correlation functions are only calculated for $-M \leqq m \leqq M$. For practical purposes, however, one can assume the correlation functions to be zero for $m + M$. The upper summation index can therefore be limited to $M - m$.

Fig. 5 shows the auto-correlation function of the output and Fig. 6 the cross-correlation function between output and input of a lag network excited by white noise. The variance for different observation length is shown. The sampling time was 0·2 sec. The lag time constant of the network is 0·5 sec. The variance is smaller with longer observations.

Unfortunately the length of the observation time is more determined by practical considerations during flight tests than by statistical requirements only. In many

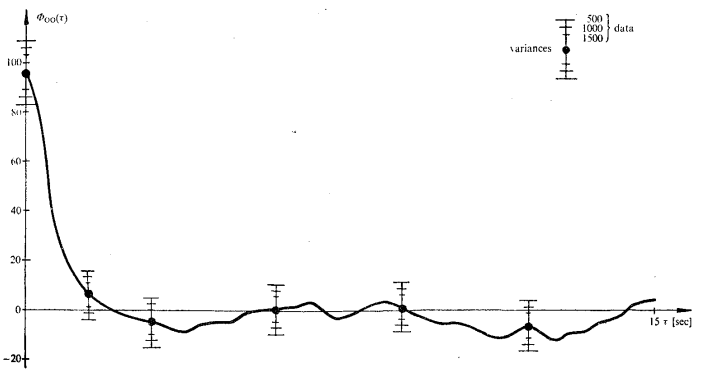

Fig. 5. Output autocorrelation function of a lag network.

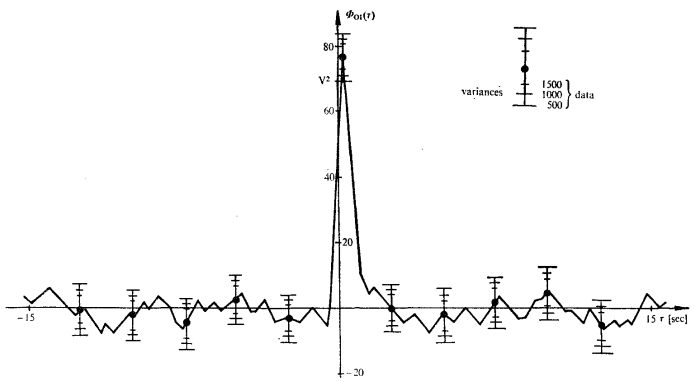

Fig. 6. Crosscorrelation function (output-input) of a lag network.

cases, however, good results are obtained even if the length of observation is not sufficient. Fig. 7 shows two correlation functions. Both have been obtained by analyzing the stick deflection of two different pilots during flight. In the second correlation function a sinusoidal component introduced by one of the pilots can be detected.

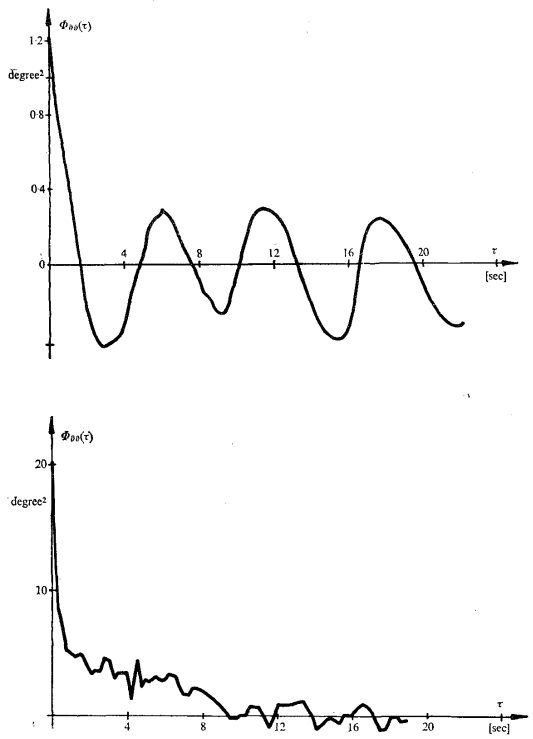

Fig. 7. Autocorrelation functions of stick deflection during hovering flight (two pilots).

Power Density Spectra. The cross power density spectrum is defined as the Fourier Transform of the crosscorrelation function

$$S_{xz}(f) = \int_{-\infty}^{+\infty} \Phi_{xz}(\tau)\, e^{-j\omega\tau}\, d\tau\,. \tag{18}$$

For evaluation the real and imaginary part have to be calculated separately

$$\text{Re}\, S_{xz}(f) = \int_{-\infty}^{+\infty} \Phi_{xz}(\tau) \cos \omega\tau\, d\tau\,, \tag{19}$$

$$\mathrm{I_m}\, S_{xz}(f) = -\int_{-\infty}^{+\infty} \Phi_{xz}(\tau) \sin \omega\tau \, \mathrm{d}\tau \,. \tag{20}$$

According to Eq. (10) it is sufficient to undergo only a cosine transformation for obtaining the auto power density spectrum

$$S_{xz}(f) = 2\int_{-\infty}^{+\infty} \Phi_{xx}(\tau) \cos \omega\tau \, \mathrm{d}\tau \,. \tag{21}$$

The integrals must be calculated numerically. As the process has been sampled at equally spaced intervals Δt, the highest signal frequency which could be detected is $f = <f_T/2 = \frac{1}{2}\,\Delta t$. Therefore, Eqs. (19)–(21) can be evaluated only for the following frequencies:

$$f_n = \frac{n}{2M} f_T \quad (-M \leqq n \leqq M) \,. \tag{22}$$

Using digital calculations for power spectra analysis, one has to consider that the correlation functions are only available at discrete time intervals. This means that one obtains due to aliasing effects all the frequency spectra

$$S_{xx}^{\triangledown}(f) = \sum_{m=-\infty}^{+\infty} S_{xx}(f - mf_T) \,, \tag{23}$$

$$S_{xx}^{\triangledown}(f) = \sum_{m=-\infty}^{+\infty} S_{xz}(f - mf_T) \,. \tag{24}$$

Evaluation power density spectra by digital means f_T has to be chosen sufficiently high so that no aliasing of the side bands can occur. Using any numerical integration method for Eqs. (19)–(21), only a raw estimate of the spectrum can be obtained because m is restricted to values $m \leqq |M|$. A good smooth of the estimate may be obtained by frequency smoothing called hamming:

$$S_{xx}(f_n) = 0{\cdot}54 S_{xx}(f_n) + 0{\cdot}23 S_{xx}(f_{n-1}) + 0{\cdot}23 S_{xx}(f_{n+1}) \,, \tag{25}$$

$$S_{xz}(f_n) = 0{\cdot}54 S_{xz}(f_n) + 0{\cdot}23 S_{xz}(f_{n-1}) + 0{\cdot}23 S_{xz}(f_{n+1}) \,. \tag{26}$$

The raw estimate of the power spectra is calculated by means of Eqs. (27) and (28) using trapezoidal integration

$$\mathrm{Re}\, S_{xz}(f_n) = \Delta t \left\{ \Phi_{xz}(0) + \sum_{m=1}^{M-1} [\Phi_{xz}(m) + \Phi_{zx}(m)] \cdot \right.$$
$$\left. \cdot \cos \frac{nm}{M} \pi + \frac{(-1)^n}{2} [\Phi_{xz}(M) + \Phi_{zx}(M)] \right\} , \tag{27a}$$

$$\text{(27b)} \qquad \operatorname{Im} S_{xz}(f_n) = \Delta t \left\{ \sum_{m=1}^{M-1} [\Phi_{zx}(m) - \Phi_{xz}(m)] \sin \frac{nm}{M} \pi \right\}$$

$$(0 \leqq m \leqq M),$$

$$\text{(28)} \qquad S_{xx}(f_n) = \Delta t \left\{ \Phi_{xx}(0) + 2 \sum_{m=1}^{M-1} \Phi_{xx}(m) \cos \frac{nm}{M} \pi + \Phi_{xx}(M)(-1)^n \right\}.$$

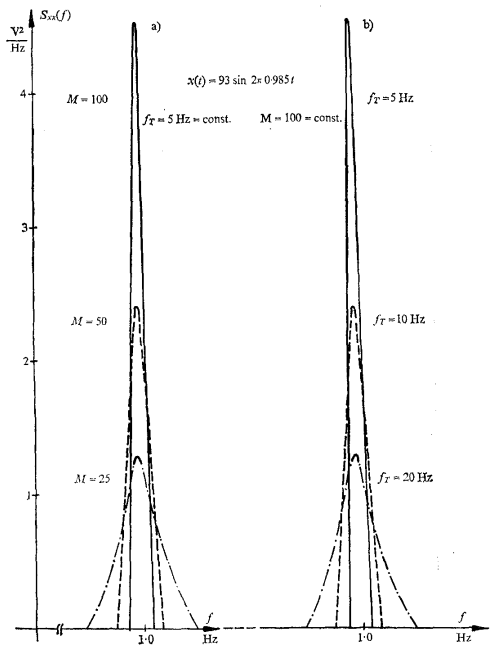

Fig. 8. Power density spectra of a harmonic. Parameters: maximum correlation time (M), sampling frequency (f_T).

Fig. 8 shows a few characteristic results. In (a) and (b) a single harmonic oscillation has been analyzed. In (a) the maximum number of correlation lag values has been kept constant to $M = 100$. The analyzed record length was 1500 samples. The sampling frequency was varied, $f_T = 5$ Hz, 10 Hz and 20 Hz. If f_T is increased, the bandwidth of the spectrum will increase according to Eq. (22). However, if M is kept constant, the number of independent spectral

estimates will be the same. That means that the intervals $\Delta f = f_T/2M$ where the spectrum is estimated are wider if f_T is increasing. In the present case with only one harmonic oscillation the energy which is constant is dissipated in a wider interval as f_T increases.

If f_T is kept constant and the maximum number of correlation lag values M is varied to values $M = 100$; 50; 25 one encounters to the same situation (Fig. 8b). Decreasing M means increasing the intervals in which the energy of the spectra is estimated. Therefore the results shown in Fig. 8 are identical because it is the same if one varies M in the ratio 4 : 2 : 1 or f_T in the ratio 1 : 2 : 4.

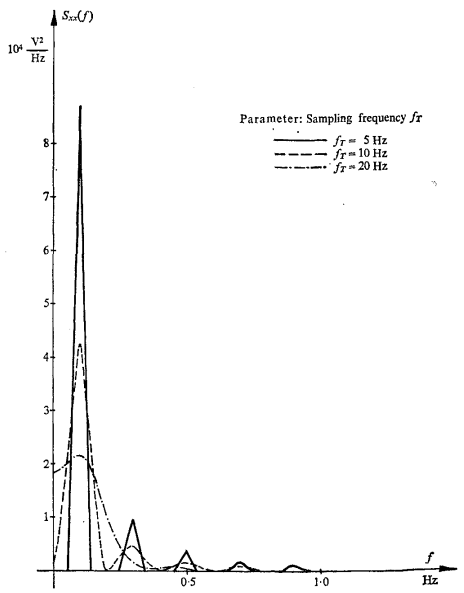

Fig. 9. Power density spectral of a square-wave (0.1 Hz).

Before analyzing a record, thoughts have to be given to how many independent spectral estimates have to be detected and to what the bandwidth will be. This is particularly true in the case of period phenomena in the spectrum.

Fig. 9 shows the analyzed spectrum of a square wave with a fundamental periodic of 0·1 Hz. The harmonic oscillations of the square wave will be 0·1; 0·3: 0·5; 0·7; ... Hz. For spectral density analysis the following sampling frequencies were chosen $f_T = 5$ Hz; 10 Hz and 20 Hz. Evaluation with $M = 100$ lag intervals yields power density estimates at intervals $\Delta f = 0{\cdot}025$ Hz; 0·05 Hz and 0·1 Hz. It is obvious from Fig. 9 that overlapping problems will increase with Δf increasing because the constant power of each single harmonic is sperad over a wider frequency range.

If the signal frequency band extends half the sampling frequency aliasing occurs. This is shown in Fig. 10 where the power density spectrum of a square-wave with a fundamental periodic of 1·5 Hz is given. Sampling with $f_T = 30$ Hz yields an unaliased power density spectrum. Strong aliasing occurs at a sampling frequency of $f_T = 10$ Hz. In this case the sampling theorem is only valid for the fundamental and the third harmonic.

To avoid aliasing the sampling frequency has to be chosen twice the highest signal frequency. A signal with unknown frequency bandwidth must be modified by a low pass filter in order to prevent aliasing effects of noise and energy rich disturbances of higher frequencies.

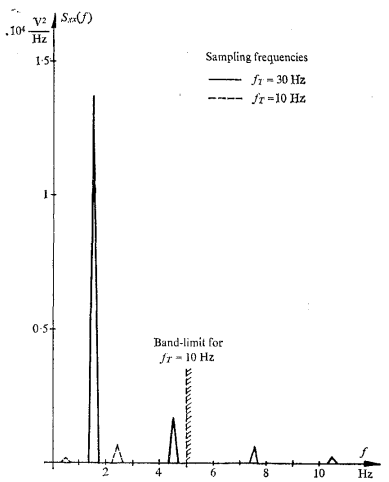

Fig. 10. Spectral density analysis of a square-wave 1.5 Hz-aliasing problems.

III. DIGITAL IMPLEMENTATION OF CORRELATION AND POWER SPECTRA CALCULATIONS

Digital implementation of correlation and power spectra calculations can considerably benefit from the use of hybrid or process control computers. There are two specific difficulties when the correlation and power spectra calculations are implemented on such a computer: The enormous number of individual digital operations to be performed and the large storage capacity needed for handling large quantities of data. In the following it will be shown how these problems have been solved on the Dornier SDS 9300 computer with a 8096 twenty-four bit memory and two magnetic tapes. This computer is mainly used for data processing and hybrid simulation.

III.1 Some Consideration on Time Optimisation

With A—D converters analog data can be quantized at 10^4 scale units; that means the computer words will have about 13 useful bits of information. As the normal computer words of the SDS computer and most of the process computers have 24 or in some cases 18 bits, one should not use double precision length which is required for floating point operations, thus increasing the computer data artificially to 48 or 36 bits, where only 13 bits are used.

Fixed point implementing of all the numerical calculations requires careful investigation during programming in order to avoid any possible overflow. There are special summing routines in the program where double-precision appears to be necessary. But even then, fixed point operations are usually considerably faster than floating point operations, e. g. in the case of the SDS 9300

addition (fixed point 24 bit word length)	3·5 μsec
addition (fixed point double precision)	5·2 μsec
addition (floating point)	10·5÷19 μsec

As the input data are principally digitalized from analog form at 10^4 scale units, one may avoid any overflow associated with the fixed point computation of the correlation and power spectra.

By inspecting the machine code program produced by a Fortran Compiler it was learned that the Fortran II compiler using double precision operation does not make full use all of the possibilities of the available instructions especially in connection with the index-registers. Therefore the whole program was written in machinecode. Investigating all the procedures with regard to minimum computer time and making full use of the three index registers, time for the overall computations could be saved. This is particularly true in the case of certain inner loops which are run very often.

III.2 Consideration on the Memory Requirements

The Fortran Compiler at hand requires 4000 24 bit memory words for the monitor. Therefore memory considerations, too, rule out the use of Fortran for programming. The length of the program written in machine code instructions with all the necessary subroutines required for the calculation of the means and variances, the probability density functions, some tests for randomness and stationarity, the correlation and power spectra functions uses roughly 4 500 twenty-four-bit-words. 3 000 words are reserved for two arrays of the digitized data of two stochastic processes. 1 500 sampled values from a weakly stationary process yields, as the experience shows enough information, provided the adequate sample interval has been chosen. The correlation functions are computed up to a maximum correlation lag value of 150.

During computation the input data are firstly normalized and possible trends are removed. After this the original data are no longer required and the storage capacity of the input data can be used for the normalized data. If the raw estimates of the correlation function have been calculated, the normalized data are no longer needed for the computations. The memory capacity can now be used for the power spectra calculations.

This technique using the memory during the different phases of the computations several times, allows the handling of large amounts of data even with a relatively small computer.

If magnetic tapes are available, the amount of data which can be handled, could be increased. So far we use one tape for data input and one tape for output. It is difficult to make assertions to the influence of the use of tapes on computer time. A rather sophisticated data organisation

for the tapes is necessary in every case in order to make full use of the computer's data transfer rate of nearly 300 000 words per second.

The use of magnetic tapes as output for the results and printing out the data later on in off-time operation, both can help to save computer time and memory capacity because all output subroutines with the one exception of the tape handling programs are no longer needed.

Some characteristic values for the computer time used with the program written at Dornier GmbH shall be given. 43 sec are used for analyzing two stochastic processes each having 1000 sample values. The correlation function values are computed for a maximum lag of 75. The program will give the following results for each of the two arrays:

means and variances,
probability density functions,
estimates for the auto correlation functions,
variance for the estimates of the correlation functions,
auto-power spectra,
estimates for the cross correlation function between the two processes,
variance for the estimates of the cross correlation function,
cross power spectrum,
amplitude and phase of the frequency response (calculated only for linear systems if necessary).

The 43 sec used for the data processing are split up into 14 sec for the effective computer time, 5 sec for the data exchange from the input of the tape into the memory of the computer and 24 sec for the on-line output of the results on the printer. One observes that considerable time could be saved by using the tapes with off-line operation for the printing as output device discussed above.

IV. PROBLEMS INVOLVED WITH THE APPLICATION OF STATISTICAL METHODS FOR IN-FLIGHT MEASUREMENTS

Statistical methods have been applied to a large extent during the investigation of the hovering mode for VTOL aircraft at the Dornier GmbH. The following methods have been used:

a) Transfer function measurements during flight for investigating the dynamics of the system and system components.

b) Transfer function measurements during flicht for detection of any malfunction of systems,

c) Measurements to investigate the main sources of disturbances.

IV. 1 Transfer Function Measurements

Stability analysis requires the determination of the open loop transfer function of the attitude-stabilized hovering rig from in-flight measurenmets (Fig. 11). The block diagram is shown in Fig. 12. As it is absolutely impossible to perform an open loop transfer function measurement with any stimuli with a plant having a double pole in the origin, the open loop transfer function was determined by measuring the

closed loop. This yields

$$F_0 = \frac{F_g}{1 - F_g} \tag{29}$$

(F_0 – frequency response of the open loop transfer function, F_g – frequency response of the closed loop transfer function).

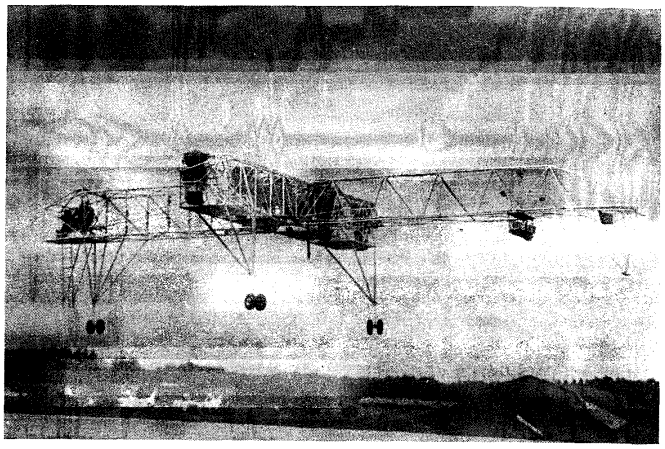

Fig. 11. Hovering rig of the Dornier GmbH.

It is difficult to ensure sufficient accuracy applying Eq. (29). It is known that a closed loop control system should be very insensitive against changes of the open loop characteristics. This means that errors of the open loop transfer function measurements will have normally only negligible effects on the accuracy of the closed loop transfer function computed by the open loop data. If it is required to determine the open loop from the closed loop transfer function, the reverse effect occurs. Any errors of the closed loop measurement are amplified if the open loop transfer function is computed with these data. This fact may be recognized by inspecting the denominator of Eq. (29) $1 - F_g$ and remembering that in the interesting frequency range F_g should be flat and equal to 1, if the control system performs nicely.

There was sufficient knowledge of the attitude control loop as to assume that the system was of a minimum phase type. The problem which had to be decided was, whether to use magnitude and phase information of the closed loop or only magnitude or phase information for the determination of the open loop. The missing phase

of magnitude can be computed by means of

$$\Phi(\omega) = \frac{1}{\pi}\int_{-\infty}^{+\infty} \frac{\mathrm{d}\ln F}{\mathrm{d}n} \ln \operatorname{ctg} h|u|/2 \,\mathrm{d}u \tag{30}$$

with

$$u = \ln \omega'/\omega ,$$

$$|F(\omega)| = |F(\infty)| - \frac{2}{\pi}\int_0^{\infty} \frac{\omega^*\varphi(\omega^*) - \omega\varphi(\omega)}{\omega^{*2} - \omega^2} \mathrm{d}\omega^* . \tag{31}$$

A theoretical investigation of the attitude control system shows that using magnitude information only will give the best results for the open loop transfer function. The reason for this fact will be explained shortly.

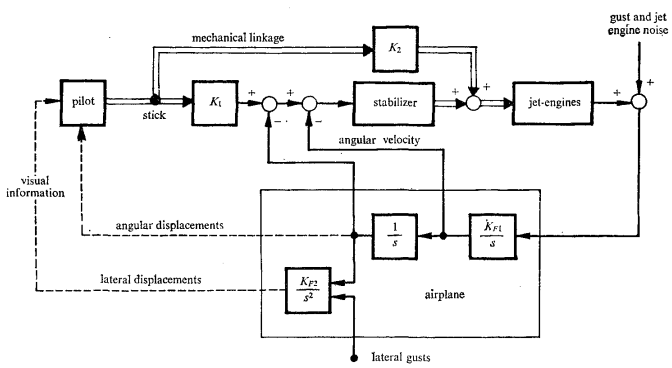

Fig. 12. Block diagram of the attitude-stabilized rig.

The open loop transfer function is determined by

$$F_0 = \frac{|F_g|\, \mathrm{e}^{\mathrm{j}\varphi_g}}{1 - |F_g|\, \mathrm{e}^{\mathrm{j}\varphi_g}} \tag{32}$$

where φ_g is phase of the closed loop transfer function.

Fig. 13 shows an illustrative example of an open loop transfer function of the attitude stabilized ring.

By partial differentiation and substitution of F_g by F_0 in an adequate form one obtains

$$\Delta F_0 = \underbrace{(1 + F_0)\, F_0 \frac{\Delta F_g}{F_g}}_{\text{I}} + \underbrace{\mathrm{j}(1 + F_0)\, F_0\, \Delta\varphi_g}_{\text{II}} \tag{33}$$

The resulting error ΔF_0 is plotted in Fig. 14. It is assumed here that $\Delta|F_g|/|F_g| = 0{\cdot}1$ and $\Delta\varphi_g = 10°$.

If one measures the magnitude one may calculate the phase φ_g with the aid of Eq. (30). The phase error due to the magnitude error of e. g. 0·1 can be computed, too. A quick look at Fig. 14 shows that the overall error ΔF_0 is considerably smaller, compared wit the measurement of both phase and magnitude.

According to this theoretical analysis and to practical experience in the majority of inflight measurements where minimum phase system could be assumed only magnitude information is used at Dornier GmbH for transfer function analysis.

Fig. 13. Open loop frequency response of the attitude-stabilized rig.

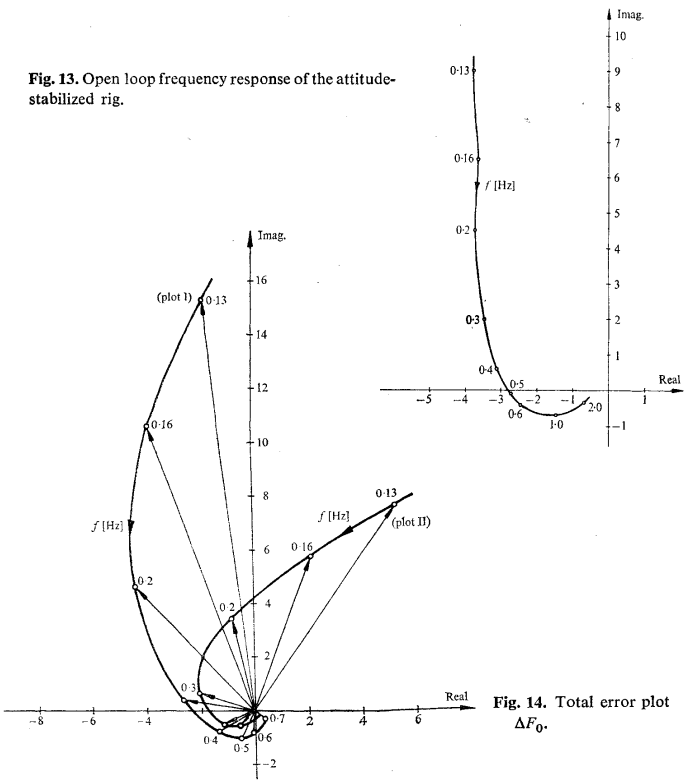

Fig. 14. Total error plot ΔF_0.

Transfer function measurements can provide a very successful tool to investigate the main sources of disturbances in a system. During the operation of the hovering rig, the nature and the source of the disturbances had to be investigated. From the

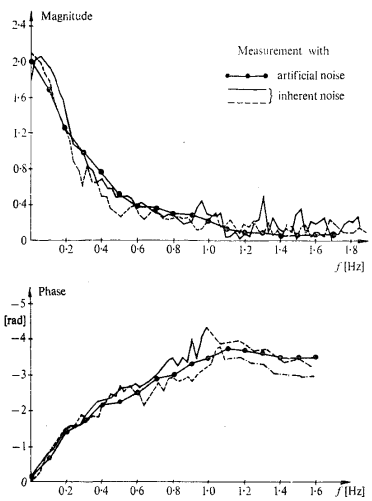

Fig. 15. Source of disturbances detection by two different measurements. Magnitude- and phaseplots of the attitude-stabilized hovering rig.

block diagram (Fig. 12) it is obvious that three major sources of disturbances will disturb the attitude control system. These are the pilot-introduced noise, the gusts and the jet engine noise. To investigate the main source of the disturbances, the following measurements have been made. The closed loop transfer function was determined by applying artificial pseudo-random signals as stimuli with the stick as input and the attitude as the output. After this, tests have been made measuring the ratio stick input to roll attitude of the closed loop without artificial stimuli by means of calculation $S_{k\varphi}/S_{kk}$. Assuming the inherent noise sources as in Fig. 12 these measurements must yield

$$\frac{S_{k\varphi}(j\omega)}{S_{kk}(\omega)} = -F_s(\omega)\frac{1 - \overline{F_p F_s}\,\dfrac{S_{\sigma\sigma}(\omega)}{S_{pp}(\omega)}}{1 + |F_s F_p|^2\,\dfrac{S_{\sigma\sigma}(\omega)}{S_{pp}(\omega)}} \tag{34}$$

(F_s – frequency response of the attitude stabilized rig, F_p – frequency response of the human operator, $S_{\sigma\sigma}$ – power spectra of the gusts and jet engine noise, S_{pp} – power spectrum of the pilot induced noise, $\overline{F_p F_s}$ – complex conjugate).

Fig. 15 shows some results. No remarkable difference between the measurements with and without artificial stimuli is observed. Therefore one can conclude that $S_{pp} \ll S_{\sigma\sigma}$.

V. CONCLUSIONS

Digital data processing of stationary stochastic processes proved to be a successful tool for in-flight measurements. Many problems could be investigated with these methods within the frame of a VTOL transport development program.

At the present time the problems of the regression analysis are studied, to investigate whether the regression analysis or the statistical methods of the control theory described here are more powerful for parameter identification.

(Received March 3rd, 1967.)

REFERENCES

[1] Bendat, Julius S., Piersol, Allan G.: Measurement and Analysis of Random Data. John Wiley & Sons, Inc., New York—London—Sydney 1966.

[2] Blackman, R. B., Tukey, J. W.: The Measurement of Power Spectra. Dover Publications, Inc., 180 Varick Street, New York 14, N. Y.

[3] Davenport, Wilbur B., Root, William L.: An Introduction to the Theory of Random Signals and Noise. McGraw-Hill Book Company, Inc., New York—Toronto—London 1958.

[4] Kreil, W., Schweizer, G.: Auswertung stochastischer Messwerte. Dornier Report No. F-5614 08, Oct. 1966; will be published in „Beihefte zur NTZ".

VÝTAH

Určování přenosů statistickými metodami s použitím číslicového počítače

W. KREIL, W. SCHNITZLER, G. SCHWEITZER

Článek je věnován problematice výpočtu statistických charakteristik náhodných procesů a jejich použití pro určování přenosů leteckých konstrukcí. Vychází se z údajů naměřených na fyzikálním systému s náhodnými komponentami. Použití číslicového počítače se diskutuje zejména z hlediska programu pro nejrychlejší zpracování údajů.

Kromě teoretického odvození a popisu metodiky článek uvádí i uspořádání experimentů a několik užitečných postřehů, které vyplynuly z praktického ověření a které autoři podložili i teoretickou úvahou.

Dipl.-Ing. W. Kreil; Dipl.-Phys. W. Schnitzler; Dr.-Ing. G. Schweitzer; Dornier GmbH, 799 Friedrichshafen, Postfach 317. DBR.